^{1}H NMR relaxation study of cellulose and water interaction in paper

DONATELLA CAPITANI, MARIA C. EMANUELE, JURAY BELLA, ANNA L. SEGRE, DONATO ATTANASIO, BONAVENTURA FOCHER, AND GEORGIO CAPRETTI

ABSTRACT

The authors studied interaction between water and cellulose in laboratory paper prepared ad hoc in alkaline condition using ^{1}H NMR relaxation techniques. Since paramagnetic substances play a major role in NMR relaxation processes, EPR spectra were also studied. ^{1}H NMR can give information on the interaction between cellulose and water coupled by a strong spin diffusion that can equalize T_1 values. Measurements of the cellulose/total water molar ratio and the cellulose/bound water molar ratio result from the free induction decay. Free water content in groundwood paper is more than double for linter and kraft paper sheets. Performing a line shape analysis of the ^{1}H resonance as a function of temperature provides information about the porosity of the system obtaining a scale of the distribution of pore diameter sizes. T_2 values of the water component depend on the amount and type of paramagnetic impurities that shorten T_2 values and the amount of free water. This parameter is therefore only useful for comparing paper from the same origin.

Application:

Using only 10–20 mg of paper, NMR relaxometry allows a precise measurement of the content of free water, bound water, and cellulose and an approximate evaluation of porosity.

PAPER PRIMARILY COMPRISES LONG fibers of cellulose. In low quality paper, this cellulose embeds in a hemicellulose and lignin matrix. In antique and laboratory prepared high quality paper, only cellulose fibers are present *(1)*. Crystalline fibers are present as polymorphs usually in the forms Iα and Iβ *(2)*. The polymorphic composition and type and relative amounts of impurities reflect the fiber origin *(3)*. Cellulose is not the only primary component. An almost equimolar amount of bound water is always present *(4)*. Researchers have studied water-cellulose interactions for many years using many techniques including moisture sorption, deuterium exchange of hydrogen in the –OH group, and infrared studies of deuterated cellulose *(5, 6)*. For all techniques, very poor information is available on the nature of the water-cellulose interface.

A measurable loss of bound water and a greater amount of amorphous cellulose always accompanies destruction of the texture of a material. Water is not present as a constituent in the crystallites of the polymorphous cellulose component *(7)*. Since strong spin diffusion is present between cellulose and water *(8)*, water domains must somehow permeate the cellulose domains and be related by a network of hydrogen bonds. The chemical approach to this problem introduces two components, i.e., free water and water bound by hydrogen bonds to the hydroxyl groups present in the cellulose. The physical approach considers water confined in the space between cellulose microfibrils.

Both chemical and physical approaches are correct but not equivalent *(9)*. We will primarily use the second viewpoint remembering that both pictures provide useful models.

The purpose of this work is to characterize the water component present in paper and find a relation between spectroscopic parameters and chemical and physical interactions relating the water and the cellulose matrices. Nuclear magnetic resonance (NMR) relaxometry is a suitable physical method for this. Since paramagnetic impurities may influence the magnetization, we also performed a careful electron spin resonance (ESR) study.

EXPERIMENTAL PROCEDURES

Materials

This study used the following commercial pulps: bleached pine kraft pulp (K), cotton linters (L), and groundwood spruce pulp (WP). The reported acronyms are the following: KN, kraft neutral sizing; LN, linters neutral sizing; and WPN, groundwood neutral sizing. K and L were soaked in water and beaten in a Valley beater to a Schopper-Riegler freeness of 28 and 30, respectively. WP pulp with a Schopper-Riegler freeness of 55 was used as received. Alkyl ketene dimer (AKD) and rosin size came from a commercial source. Antique paper was from C. Federici, Ist. Centrale per la Patologia del Libro. The paper used in this work came from an unprinted fifteenth century sheet from northern Italy. It had perfect texture and color. Similar to most paper sheets of that age, its composition is entirely flax. To mimic real paper and have better control of moisture in this study, we chose to work on sized paper.

Thermal aging used a regulated oven at 90°C and 65% RH. The various aging times used are indicated whenever necessary.

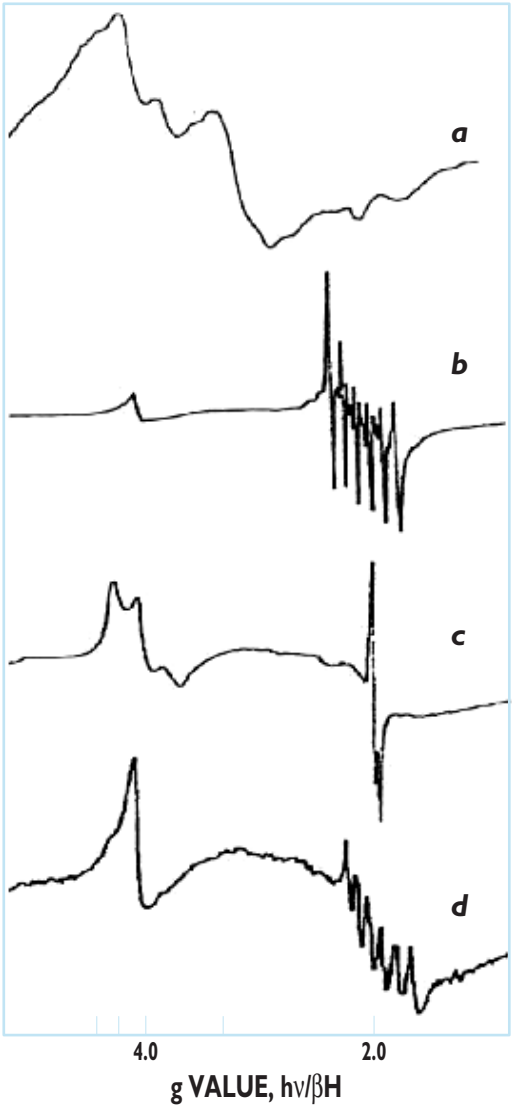

1. 110 K, X-band ESR spectra of various samples of commercial paper sheets illustrating the spectral diversity exhibited by these materials

Methods

Cellulose in microcrystalline powder form came from a commercial source without any treatment. Neutral sizing used commercial AKD. The synthetic size (1.3% o.d. pulp) was added to the fiber stock at 0.6% consistency containing calcium carbonate filler (10% a.d. pulp) at pH 8.0.

Handsheets prepared in laboratory standard form used TAPPI T 205 method with air drying and heating 10 min at 378K. The degree of sizing measurement used TAPPI T 441 giving the following results: KN, 25.0 g/m^2; LN, 30.0 g/m^2; and WPN, 17.5 g/m^2. To keep free water as low as possible without causing any damage to the paper texture *(10)*, we kept our handsheets in a dry atmosphere of 23°C and 50% RH.

ESR. The spectra were recorded at X-band frequency of approximately 9.1 GHz at approximately 100K for a better signal to noise ratio using a commercially available spectrometer with a standard variable temperature accessory. When necessary, field and frequency were measured with a commercially available gaussmeter and counter, respectively. All samples had comparable weights of about 30 mg. Their height remained within 5 mm so they were well within the maximum sensitivity region of the instrument cavity. Paramagnetic ion concentrations were measured by comparing the signal areas with appropriate calibration curves according to a procedure already reported *(11)*. Estimation of the total errors was within 10%.

NMR. Samples of the laboratory prepared handsheets kept at controlled atmosphere of 23°C and 50% RH were introduced into 5 mm NMR tubes and then sealed. To keep the paper samples well within the NMR receiver coil, the height of samples was approximately 0.5 cm. The weight of each sample was 25.0 mg. The 90° pulse was 3.8 μs. The dead time of the instrument was 8 μs. All measurements were performed from high to low temperature. Repeated measurements used a freshly prepared sample. All T_1 measurements were performed at 57 MHz. T_1 relaxation times over the full temperature range were measured as previously reported *(4)*. Line shape data were collected at 57 and 81 MHz. For this purpose, free induction decays (FID) were obtained in quadrature detection with a scan size of 2K words. Fourier transformation was performed after zero filling and a modest exponential multiplication. A 2K time domain was always used with a repetition time longer than at least five times T_1. For the determination of the ratio between the sharp component and the total signal, at least 64 scans were allowed. Approximate T_2 values of the water component were obtained directly from the line width measured at half height *(12)*. Data analysis was performed as previously described *(4, 13)*.

RESULTS AND DISCUSSION

At temperatures higher than 200K, the proton free induction decay of any sample of paper always shows two components. One is a rapidly decaying component due to the cellulose. The other is a slower decaying component from the water. Performing T_1 measurements on both components is possible *(14)*. As previously shown *(4)*, the molar ratio between water and cellulose can be obtained by performing a careful analysis of the FID in the time domain.

By lowering the temperature, the water resonance progressively broadens. At approximately 200K, it disappears into the broad cellulose resonance. This process is so slow and continuous that it allows the determination

of many parameters related to the water mobility and its interaction with cellulose domains.

As previously shown, the water and cellulose components exhibit multiple spin-lattice relaxation so that different T_1 values can be measured. In agreement with the presence of paramagnetic centers, the shortest experimental T_1 values are a few milliseconds. They clearly point to a relaxation mechanism dominated by the presence of paramagnetic impurities.

Note that several complementary types of information are available from different magnetic resonance measurements that will have separate discussions. The discussion will also explain the nature and origin of paramagnetism in paper

Data about long-range bulk properties obtained from T_1 measurements are already available *(4)*.They will only be mentioned and not discussed.This paper will present NMR data regarding local properties about the bulk material but concerning short-order compartments and extracted from T_2, the FID, or the line shape itself. To be exhaustive from $T_{1\rho}$ measurements (the spin-lattice relaxation in the rotating frame *(14)*), additional work will examine the possibility of obtaining information concerning intermediate distances.

ESR properties

Samples of commercial or laboratory prepared paper either new or aged generally exhibit complex and widely differing spectra where several paramagnetic centers such as transition metal ions, organic free radicals, and paramagnetic point defects can be easily detected. A full analysis of these are available elsewhere *(15)*. Here a short, qualitative description will describe only the fast relaxation mechanisms detected by NMR methods.

Paper spectra in **Fig. 1** indicate that trivalent iron present as ferromagnetic impurities or in pseudo-octahedral, axial, or rhombic environments is the most common paramagnetic impurity with concentrations up to 500–700 ppm. Mn^{2+} and sometimes Cu^{2+} are also present in paper although usually at concentrations below 100 ppm. In laboratory-made handsheets, a sharp free radical line ($g = 2.0034, \Delta H_{pp} = 1.5–11$ gauss) commonly occurs due to the presence of lignin or organic fillers used in the manufacturing process. Finally, complex point defect spectra may occur. They consist of an oxygen peroxy-type radical and an A1-centered defect. Some paramagnetic centers are intrinsic impurities because they are already present in raw wood material. Some defect centers are entirely due to the presence of kaolin. This is an aluminum silicate of approximate formula $Al_2O_3 \cdot 2SiO_2 \cdot H_2O$ used as a filler.

In Fig. 1, spectrum a (newspaper) is dominated by ferromagnetic impurities, but Mn^{2+} and a small amount of rhombic Fe^{3+} are the most prominent features of spectrum b (white paper for photocopy). A more intense and split iron signal is present in sample c (modern printing paper containing lignin) with a complex free radical feature at g = 2.0. Finally, spectrum d (air mail light paper) exhibits sizeable amounts of Mn^{2+} and rhombic and pseudo-octahedral Fe^{3+}.

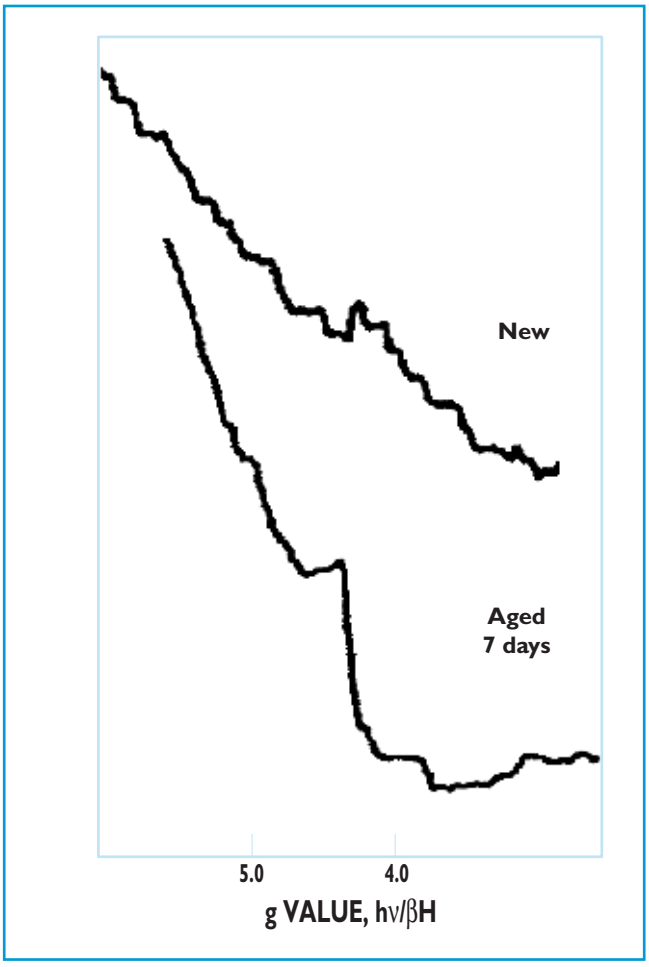

2. 110 K, X-band ESR spectrum of a laboratory sample of kraft paper showing the increase of rhombic Fe^{3+} content upon thermal aging at 90°C and 65% RH for seven days showing only the region around g = 4.3

We have previously shown that paramagnetic impurities play a key role in the degradation of paper by acting as catalysts and initiators of hydrolytic, oxidation, or both reaction sequences. These lead to the depolymerization and amorphization of cellulose *(8)*. Closely connected is the observation that the paramagnetic centers undergo profound changes upon thermal or photochemical aging of paper. A particularly interesting example of such transformations is the increase in concentration of the rhombically symmetrical Fe^{3+} upon thermal aging of **Fig. 2**. Since Fe^{3+} in this specific stereochemistry is the most active hydrolysis catalyst, paper degradation may reasonably be a two-step process. In the process, the onset of

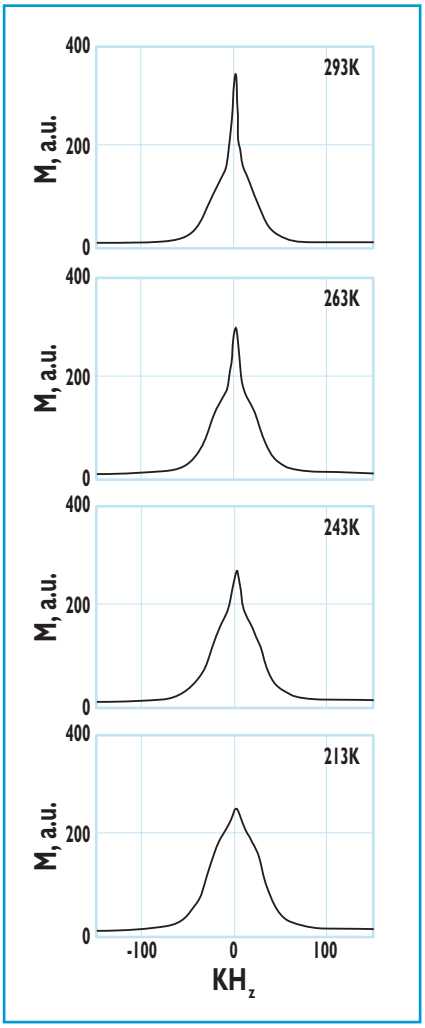

3. ^{1}H NMR spectra at 81 MHz as a function of the temperature for a sample of groundwood paper with the water line progressively disappearing but still observable down to 213K

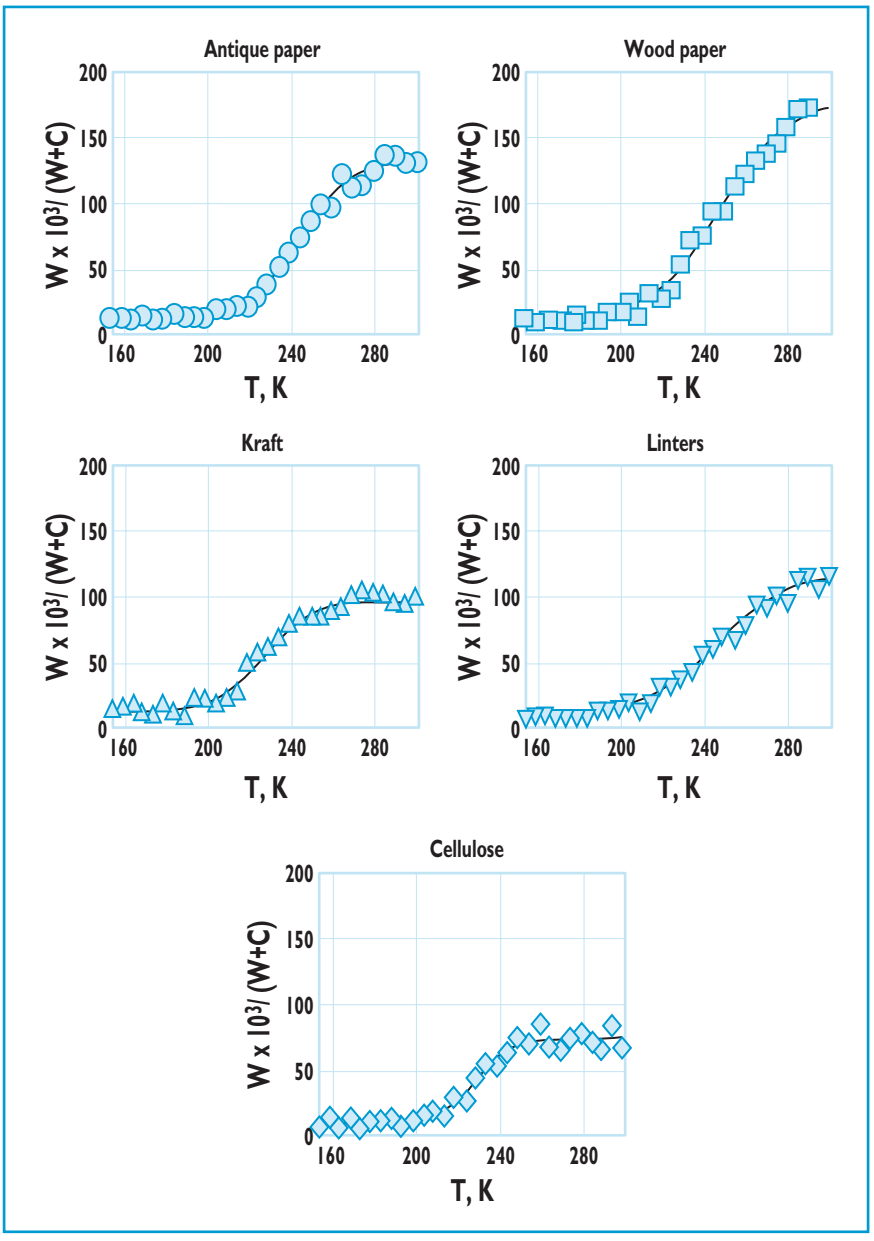

4. Plot of the ratio (equivalent weight in protons) between the magnetization of mobile water and the total magnetization (mobile water plus frozen water plus polymeric materials) as a function of temperature

the hydrolytic reaction sequence is preceded by activation of the catalyst, i.e., migration of the paramagnet to a proper chemical and geometrical environment induced by aging.

Long range properties: T_1. The extreme T_2 difference between water and cellulose can provide separate relaxation parameters for both components *(8)*. Using an instrument with a short dead time and choosing the initial part of the FID, T_1 relaxation can be measured for the cellulose component alone. Allowing a dead time of more than 50 µs and measuring only the slow decaying component, T_1 relaxation can be obtained for the water component. Previous work shows that for the water and the cellulose components more than one T_1 value can be measured. These values relate to a fraction poor in paramagnetic impurities and to another (or more than one) rich in paramagnetic impurities. We chose to ignore this last fraction characterized by short T_1 relaxation *(16)*.

If a composite material has large domains, the spin diffusion process will not be fully active. Different components will therefore show different T_1 relaxations. If a fully interpenetrating network of domains is present, the spin diffusion process will equalize T_1 values *(17)*.

This is the case of the paper as previously reported.The spin diffusion process is fully active between the water and the cellulose domains *(8)*.

As previously shown, the most significant parameter related to long-range properties is the activation energy of the total motion of the sys-

tem of cellulose and water. The bulk magnetic response correlates to the onset of molecular motions. These are then responsible for mechanical and dielectric losses *(18)*. T_1 relaxation study as a function of the temperature is very useful to determine local motions and properties of synthetic polymers. Such measurements were recently performed on wood *(19)*, cotton *(20)*, and paper *(4)*.

Short range properties: T_2, FID, line shape. By lowering the temperature from ambient to approximately 220K, the water peak progressively disappears into the broad resonance due to the cellulose as **Fig. 3** shows. Analyzing the total amount of mobile water, one can see that the first water to disappear is "free water." In groundwood pulp paper going from 300K to 263K, a large loss on the water signal occurs as Fig. 3 shows. This loss is much smaller in all other samples (kraft, linter, and antique paper) confirming our previous observation *(4)* that the amount of free water in antique paper or in laboratory handsheets of very high quality is very low.

Consider paper as a porous system containing a mobile species or water embedded into a rigid matrix of cellulose. This model is very crude, but it allows useful comparison with other better characterized porous systems *(9)*.

For the sake of clarity, returning to the original treatment is useful. The physical properties of a liquid confined within small pores can be radically different from those of the bulk material *(21, 22)*. The freezing point especially is lower *(23)*. This is the phenomenon that we used to characterize pore size distribution in paper by magnetic resonance spectroscopy.

According to this model, we can consider the physical model of paper, i.e., a matrix of cellulose embedded by pores of different sizes that all contain water.

The melting temperature of any liquid relates to pore size distribution *(24)*. Following a previous treatment *(9)*, the Gibbs-Thompson equation gives the relationship between the temperature reduction, ΔT_m, of the melting point of a crystalline solid confined within a pore and the pore diameter *(24)* assuming the contact angle between liquid, solid, and pore wall is 180°:

$$\Delta T_m = T_m - T_m(x) = 4\sigma T_m/(x\Delta H_f \rho) \quad (1)$$

where

σ is the surface energy at the liquid-solid interface
T_m is the normal melting point of the bulk material
$T_m(x)$ is the melting point of a crystal of linear dimension x
ΔH_f is the bulk enthalpy of fusion
ρ is the density of the solid.

For a particular liquid, the equation becomes the following:

$$T_m = T_m(x) = k/x \quad (2)$$

In differential form, this is the following:

$$dT_m(x)/dx = k/x^2 \quad (3)$$

where

k is a characteristic of the liquid.

For a porous material saturated with liquid, the melting temperature of the liquid, $T_m(x)$, relates to the pore size distribution by the following:

$$dv/dx = [dv/dT_m(x)][dT_m(x)/dx] \quad (4)$$

From Eq. 3, substituting $dT_m(x)/dx = k/x^2$ in Eq. 4 gives the following:

$$dv/dx = dvk/dT_m(x)x^2 \quad (5)$$

The measurement of $dv/dT_m(x)$ results from analyzing the amount of sharp line, i.e., a line with a very long spin-spin relaxation time, T_2, of the liquid present in the pores. This amount is somehow proportional to the total pore volume. With a lower temperature, water confined in larger pores disappears. Only water confined in pores smaller than a given dimension still gives a sharp resonance. In work in progress, we will use Eq. 5 with these data to obtain the relative pore volume as a function of pore diameter. We will also determine the pore size distribution function.

By lowering the temperature until the water signal completely disappears into the cellulose broad resonance, two kinds of data will result. As a function of the temperature, we can plot the amount of the water signal vs. the total NMR signal for water plus cellulose. This is a measure of the magnetization due to the amount of mobile water for the total magnetization. **Figure 4** shows these data. The solid line in the figure connecting the experimental points is the theoretical sigmoidal curve and results from a best fit procedure. In the 200K–265K temperature range, a slope occurs that shows the amount of water confined in pores below a given dimension.

As a function of 1000/T, we can plot the line width of the water component or its reciprocal that is proportional to T_2. This gives direct information on water mobility as **Fig. 5** shows. Since paramagnetic impurities play a major role in shortening T_1 and T_2, these T_2 values are significant only within the same family of samples. In samples containing the same paramagnetic impurities *(25)* and without free water, i.e., at temperatures lower than approximately 268K, T_2 gives a direct measurement of the water mobility.

Figure 4 shows the ratio between the magnetization of mobile water and the total magnetization, i.e., frozen water plus cellulose. For all

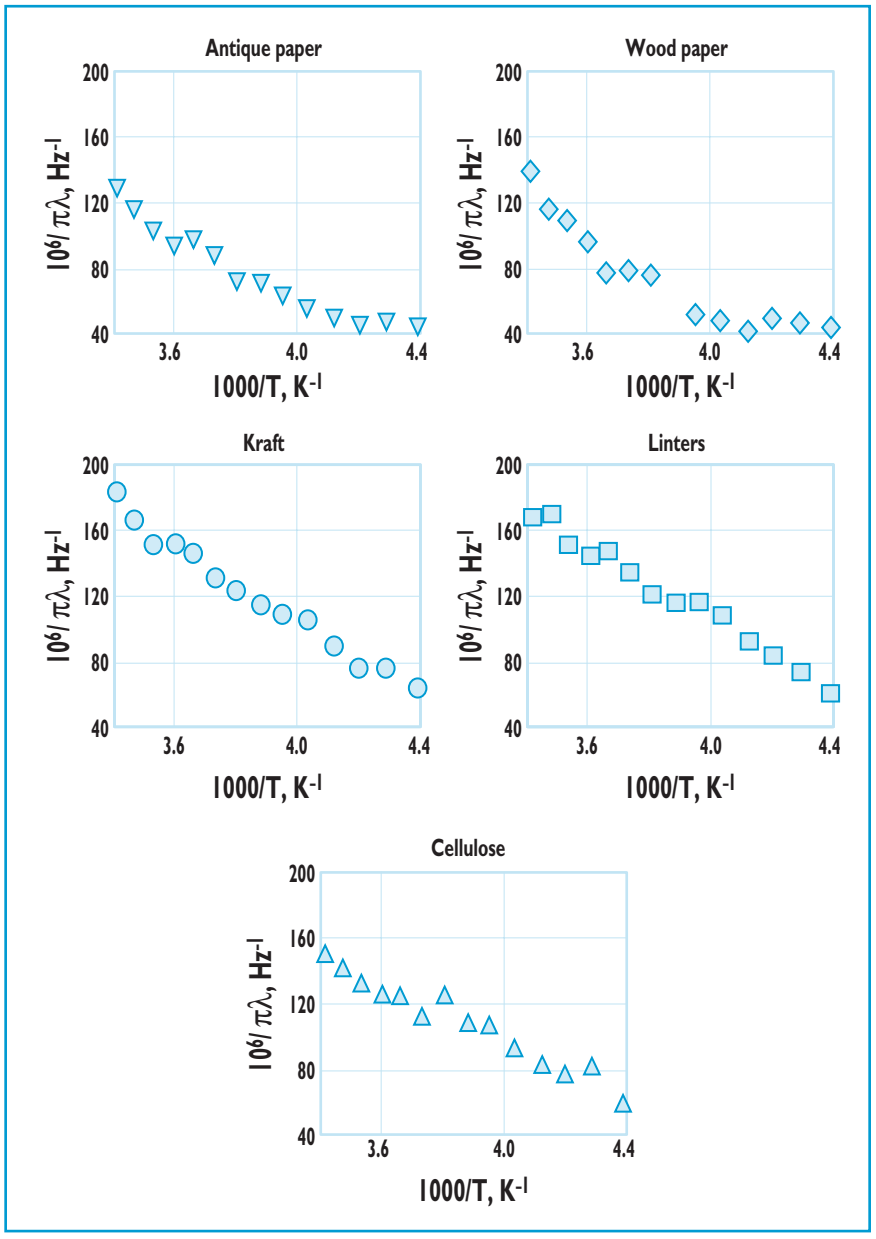

5. ^{1}H NMR at 81 MHz, T_2 in μs vs. 1000/T in all samples for a) antique paper, b) groundwood paper, c) kraft pulp, d) cotton linters, and e) cellulose with T_2 value obtained from the line width ($\Delta\lambda$) of the water component, T_2 approximately $10^6/\pi\Delta\lambda$

samples between 150K and 190K, all water is frozen. In the 200T–265K range, a slope occurs that is different for all systems. This slope relates to the amount of water confined in pores below a given dimension. For systems with a well-defined porosity, note that we would expect an almost horizontal line followed by a steep, well-defined sigmoidal curve. A high, well-defined slope is characteristic of a small range of diameters, and a small slope has the precise meaning of a large spread in the diameter of pores. A real distinction and the presence of well-defined steps can occur only when the diameter of pores is very large. In paper samples that do not present large porosities, one should expect a large distribution for small pores and the absence of large porosities.

Antique paper even if made by skillful craftsmen therefore shows an apparent spread of pore diameters larger than that of industrially made linter paper. This observation can be due to the presence of large inter-fiber holes.

The spread of pore diameter can be due to aging. For example, freezing of water in the system can cause defects. Note that the total appearance of our antique sheets is extremely good. It is also white and has the typically strong texture of antique, well-preserved paper.

Groundwood pulp paper also shows the presence of large pores probably related to the lignin fraction. These increase the apparent spread of pore diameters. A titration curve corresponding to known diameters is not available. At approximately 265K–270K, a modest plateau occurs. This corresponds to the freezing point of free water. According to previous data *(26)*, this plateau is followed by the onset of free water. The content of free water is very modest in antique paper and in linters. It is zero in dry cellulose. In paper from wood pulp, free water constitutes more than one-third of the total water.

A possible mathematical representation of the above description can result from a sigmoidal curve whose standard equation is the following:

$$y = y_0 + \{a[1 - \exp(-c(x - x_0))]\}/[b - (b - 1)\exp(-c(x - x_0))] \quad (6)$$

where

y_0 is the mean value of the plateau at low temperature
x_0 is the lowest temperature T = x_0 = 153K
a, b, and c are variable parameters to be fit respectively representing a = vertical distance between the two asymptotic values and b and c values are proportional to the first derivative of the function before and after the inflection point.

With this equation, one can obtain a reasonable fit for all our sam-

ples as Fig. 4 shows. **Table I** gives the relative parameters obtained from a best-fit procedure *(13)*. In each parameter of the table, the error is less than 10% of the actual value. In the table, y_0 is the mean value of the plateau at low temperature, x_0 is the lowest temperature T = x_0 = 153K, and a, b, and c are variable parameters requiring fit.

Note that while one can compare all data regarding any type of paper, the corresponding values from the cellulose sample are completely different. They are not a subject of discussion here.

For all our paper samples, we calculated the first derivative of Eq. 5 in the experimental point of inflection. This gave a series of P values defining the slope for each sigmoidal curve.

Even without a titration curve, one can define an easily-measurable quantity, P (slope), proportional to the spread of the diameter of pores at the inflection point as Table I shows. In high quality paper, P is small. It increases markedly in paper made with wood pulp. The parameter, P, can therefore correlate to paper type. Note that P is bound not only to the intrinsic merit of the starting material but also to the technical procedure used in paper making. The following scale reflects all previous qualitative discussions: $P_{linters} < P_{kraft} < P_{antique} < P_{groundwood}$. The main advantage of NMR measurements is that they require only a very small amount of material without staining or other cumbersome procedures.

In samples with the same content of paramagnetic impurities, T_2 is a direct measurement of the water mobility. As a function of 1000/T, Fig. 5 shows the definition of a range of water mobilities. In paper of a different kind, very different slopes are observable. Since T_2 intrinsically decreases, lowering the temperature does not give a plateau. In paper with an inherently high quality, the difference in T_2, i.e., the line width between 223K and 263K, is much lower than in paper containing lignin and hemicelluloses. Our next effort will be a titration of pore diameters measuring solids with known porosity filled with water.

Parameter	Antique paper	LN	WPN	KN	Cellulose
y_0	13	11	10.5	10.5	9.8
a	6.9×10^{-2}	4.5×10^{-1}	4.8×10^{-1}	8.0×10^{-2}	3.9×10^{-3}
b	5.8×10^{-4}	4.2×10^{-3}	2.8×10^{-3}	9.5×10^{-4}	1.3×10^{-1}
c	8×10^{-2}	6×10^{-2}	6×10^{-2}	10×10^{-2}	1.3×10^{-1}
P	2.5	1.6	2.7	1.9	2.0

I. Parameters obtained from the best fit procedure for the values of the ratio between the magnetization of mobile water and the total magnetization vs. T with a sigmoidal curve

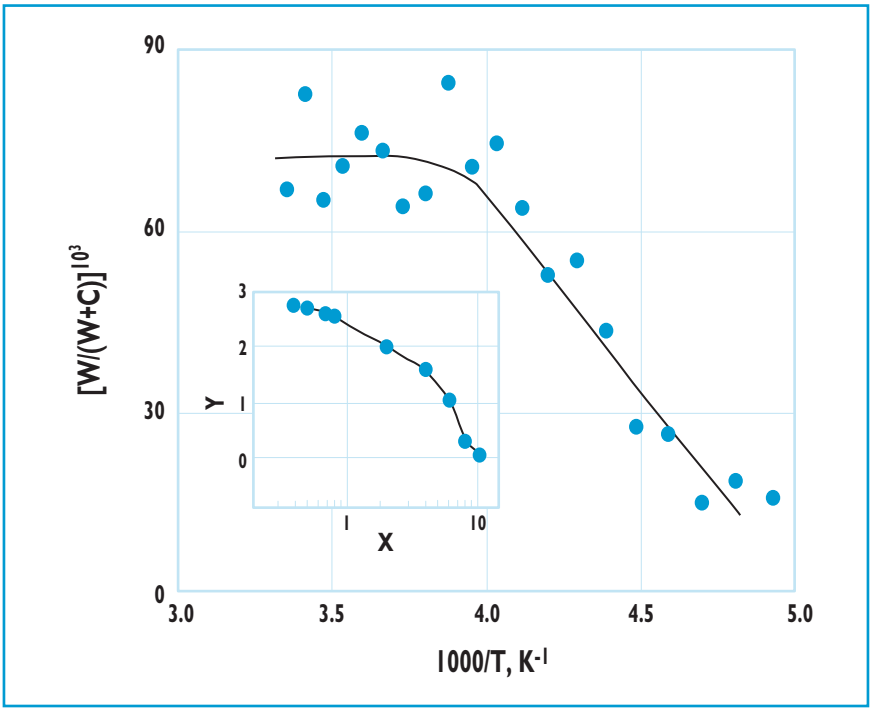

6. Cellulose sample showing a plot of the ratio (equivalent weight in protons) between the magnetization of mobile water and the total magnetization (mobile water plus frozen water plus cellulose) as a function of 1000/T

CONCLUSION

We performed an NMR relaxometric study on paper that focused on cellulose and water interactions. Cellulose and water separately observable in the FID are related by a strong spin diffusion process that equalizes T_1 values. Starting from a sufficiently low temperature, we have previously shown that T_1 as a function of 1000/T defines the activation energy (Arrhenius term) for the total motion of cellulose and water. This energy relates to the packing of cellulose fibers. In this way, one can obtain a factor related only to the physical properties of the material. From the FID itself, we obtained the measurements of the cellulose/total water molar ratio and the cellulose/bound water molar ratio *(4)*. The water content in groundwood paper is almost double that in the linters and kraft paper sheets.

From a line shape analysis of the ^1H resonance as a function of temperature, one can obtain information about the porosity of a system giving a scale concerning the presence of

large pores: $P_{linters} < P_{kraft} < P_{antique} < P_{groundwood}$. T_2 values as a function of temperature confirm the above findings.

We are aware that the necessary spectroscopic titration of porosities might be extremely difficult. This subject will be part of our next effort in the NMR characterization of paper. A possible approach to obtain a porosity titration may be to determine pore size distribution using inverse size-exclusion chromatography *(10)*. We could compare the NMR method directly with literature data obtained on a commercial cellulose. Then we could redraw the plot concerning the cellulose shown in Fig. 4. **Figure 6** shows this for the melting curve of bound water plotted against 1000/T. This would provide a striking similarity between our porosity curve for cellulose of Fig. 6 and the curve showing the cumulative accessible pore volume plotted against pore radii for cellulose in the insert *(10)*. **TJ**

Emanuele, Bella, Capitani, and Segre (corresponding author) are post-doctoral students, researcher, and director of research, respectively, at Istituto di Strutturistica Chimica and NMR Service, CNR, Area della Ricerca, M.B. 10, 00016 Monterotondo Staz., Rome, Italy. Attanasio is first researcher at Ist. Chimica Materiali, CNR, Ara della Ricerca, M.B. 10, 00016 Monterotondo Staz., Rome, Italy. Focher and Capretti are director and researcher, respectively, at Staz. Sperimentale Cellulosa e Carta, Pza. L. da Vinci, 20133 Milano, Italy.

Acknowledgement: This work received partial support by a special ad hoc program, "Technology Applied to Culture Heritage."

Received for review Nov. 13, 1997.
Accepted Nov. 17, 1998.

LITERATURE CITED

1. Roberts, G. A. F. in *Paper Chemistry* (G. A. F. Roberts, Ed.), Chapman Hall, Glasgow, 1991, pp. 9–24.
2. Atalla, R. H. and VanderHart, D. L., *Science* 17(4633):283(1984), Sugiyama, J., Vuong, R., and Chanzy, H., *Macromolecules* 24(14):4168(1991), and Kroon-Batemburg, L. M. J. and Kroon, J., *Carbohydrates in Europe* 12(1):15(1995).
3. Torri, G. Sozzani, P., and Focher, B., in *From Molecular Materials to Solids* (F. Morazzoni, Ed.), Polo Editoriale Chimico, Milan, 1993, vol. 83, p. 71.
4. Capitani, D., Segre, A. L., Attanasio, D., *et al., TAPPI J.* 79(6):113(1996).
5. Jeffries, R. *J. Applied Polymer Science* 8(3):1213(1964).
6. Knight J. A., Lamar Hicks, H., and Stepheens, K. W., *Textile Research J.* 4(2):324(1969).
7. Chanzy, H. and Herissat, B., *FEBS Lett.* 184(2):285(1985).
8. Paci, M., Federici C., Capitani D., *et al., Carbohydrate Polymers* 26(2):289(1995).
9. Strange, J. H., Rahaman, M., and Smith E. G., *Phys. Rev. Lett.* 71(21):3589(1993) and Watanabe, T., Murase, N., Staemmler, M., *et al., Magnetic Res. in Medicine* 27(1):118(1992).
10. Berthold, J. and Salmen, L. J., *Pulp and Paper Science* 23(6):J245(1997).
11. Attanasio, D. Capitani, D., Federici, C., et al., Archaeometry 37(2):377(1995).
12. Meiboom, S. and Gill, D., Rev. Sci. Instr. 29(3):688(1958).
13. Press W. H., Teukolsky S. A., Flammery B. P., *et al., Numerical Recipes. The art of Scientific Computing*, Cambridge Univ. Press, Cambridge, 1988, p. 430.
14. McBrierty, V. J. and Packer, K. J., *Nuclear Magnetic Resonance in Solid Polymers*, Cambridge Univ. Press, Cambridge, 1993, p. 42.
15. Attanasio, D., Capitani, D., and Emanuele, M. C., *Symposium Proceedings,* Materials Research Society, Warrendale, 1997, p. 387.
16. Attanasio, D., Capitani, D., Federici, C., *et al., Sci. and Techn. for Cult. Heritage* 5(1):37(1996).
17. Lowe, I. J. and Gade, S., *Phys. Rev.* 156(3):817(1967).
18. McCall, D. W., in *Relaxation in Solid Polymers* (R. S. Carter and J. J. Rush, Eds.), Special Publication 301, National Bureau of Standards, Washington, 1969.
19. Li, T. Q. Henriksson, U., Eriksson, J. C., *et al., Langmuir* 8(2):680(1992).
20. Mackay, A. L. Tepfer, M., Taylor, I. E. P., *et al., Macromolecules* 18(6):1124(1985).
21. Ailion, D. and Slichter, C. P., *Phys. Rev.* 137(2):A235(1965).
22. Awaschalon, D. D. and Warnock, *J., Phys. Rev.* B35(13):6779(1987) and Warnock, J., Awaschalon, D. D., and Schafer, M. W., *Phys. Rev. Lett.* 57(14):1753(1986).
23. Gibbs, J. W., *Collected Works*, Longmans, Green, New York, 1928, p. 252.
24. Jackson, C. L. and McKenna, G. B., *J. Chem Phys.* 93(12):9002(1990).
25. Banci, L., Bertini, I., and Luchinat, C., *Nuclear and Electron Relaxation*, VCH, New York, 1991, Appendix K.
26. Attanasio, D., Capitani, D., Federici, C., *ACS Symposium Series*, ACS, Washington, 1995, p. 332.